Intersubband transitions in dilute (In,Ga)(As,N)/(Al,Ga)As multiple quantum wells analyzed within a three-band k·p model

M. Giehler,* R. Hey, P. Kleinert, and H. T. Grahn
Paul-Drude-Institut für Festkörperelektronik, Hausvogteiplatz 5–7, 10117 Berlin, Germany
(Received 5 August 2005; revised manuscript received 17 November 2005; published 27 February 2006)

We study the influence of nitrogen (N) on the intersubband absorption spectra of dilute (In,Ga)(As,N)/(Al,Ga)As multiple quantum wells (MQWs). For MQWs with 6 nm well width and $Al_{0.33}Ga_{0.67}As$ barriers, the main absorption band at 1365 cm^{-1} exhibits with increasing N content a slight redshift in contrast to an expected blueshift, a remarkable decrease of the intensity, and a strong asymmetric broadening on the high-frequency side. In addition, a minor absorption feature appears on the high-frequency side. For MQWs with 3 nm well width and $Al_{0.42}Ga_{0.58}As$ barriers, the strong asymmetric main absorption band at 1820 cm^{-1} exhibits with increasing N content a blueshift, a decreasing intensity, and a minor absorption feature on the low-frequency side, which cannot be attributed to an intersubband transition by only taking into account the effect of N on the discontinuity of the conduction band edges in the MQWs. We analyze the transition energies within a three-band $\mathbf{k}\cdot\mathbf{p}$ band-anticrossing model for heterostructures. Because of the presence of the localized N state in the quantum well, a set of N-like states is formed in each quantum well due to the confinement. These N-like states couple to the original quantum well states, and mixed subbands are formed. The dependence of the calculated wave numbers for bound-to-bound as well as bound-to-continuum intersubband transitions on the nitrogen content are in good agreement with the experimental data.

DOI: 10.1103/PhysRevB.73.085322 PACS number(s): 78.30.Fs, 73.21.Fg, 78.67.De, 42.55.Px

I. INTRODUCTION

The incorporation of small amounts of nitrogen on anion sites in III-V semiconductors leads to a remarkable reduction of the band gap (E_G), which makes such alloys technologically important for optoelectronic devices for wavelengths between 1.3 and 1.55 μm. The reduction of E_G is well described within the so-called two-band $\mathbf{k}\cdot\mathbf{p}$ band-anticrossing (BAC) model introduced by Shan *et al.*[1] The Hamiltonian of this model takes into account the coupling between the extended states at the conduction band edge E_C[GaAs] of GaAs at Γ and the localized nitrogen (N) state at E_N above E_C. This coupling causes the formation of two mixed conduction subband branches at E_+ and E_-, which exhibit an anticrossing behavior. The redshifted lower branch at E_- is responsible for the decrease of the energy of the conduction band edge and the strong increase of the effective mass of the conduction-band electrons in Ga(As,N). O'Reilly and Lindsay[2,3] have proposed an extended version of the BAC model, which is based on a three-band $\mathbf{k}\cdot\mathbf{p}$ approximation and includes, besides the coupling between the conduction band edge and the averaged N-state, also the valence band edge of GaAs at Γ. Therefore, this three-band BAC model already takes into account nonparabolicity effects in GaAs leading to more confined states at a given width of a quantum well than predicted by the two-band model. Furthermore, this three-band $\mathbf{k}\cdot\mathbf{p}$ model shows that E_V remains nearly unaffected. Therefore, the band offset between GaAs and Ga(As,N) changes only the conduction band edge E_C, which decreases with increasing N content, causing an increasing conduction band offset $\Delta E_C = E_C$[GaAs] $- E_C$[Ga(As,N)] in Ga(As,N)/GaAs multiple quantum wells (MQWs).

On the one hand, interband transitions in thick layers of dilute Ga(As,N) and in Ga(As,N)/GaAs heterostructures have been frequently studied.[4] On the other hand, the increase of ΔE_C in Ga(As,N)/(Al,Ga)As heterostructures should be of comparable technological importance for optoelectronic devices for the mid-infrared region as the reduction of E_G for near-infrared optoelectronic devices. For instance, in Ga(As,N)/(Al,Ga)As quantum-cascade lasers, an increasing ΔE_C should reduce leakage currents from the upper laser level into other levels including continuum states and, therewith, improve the performance of such lasers. However, there are only a few reports by Guzmán *et al.*[5] and Duboz *et al.*,[6] who studied the influence of N on intersubband transitions (ISTs). Moreover, in these investigations, the experimental data were analyzed only within the simplified two-band BAC model, i.e., only by taking into account the increasing band offset with increasing N content and not the coupling between the N states and the conduction band.

In this paper, we investigate the influence of N on ISTs in dilute (In,Ga)(As,N)/(Al,Ga)As and Ga(As,N)/(Al,Ga)As MQW structures. The experimental results are analyzed within a three-band $\mathbf{k}\cdot\mathbf{p}$ BAC model for heterostructures, where we focus on the IST energies. The paper is organized as follows: In Sec. II, the samples and the experimental setup are described. The intersubband absorption (ISA) spectra are presented in Sec. III. In Sec. IV, the three-band $\mathbf{k}\cdot\mathbf{p}$ BAC model for ISTs in heterostructures is described. This model is applied in Sec. V to analyze the experimental spectra focusing on the transition energies of the ISA bands. Finally, we summarize the results and conclude in Sec. VI.

II. SAMPLES AND EXPERIMENTAL SETUP

In order to study the influence of nitrogen on ISTs, we have measured the ISA spectra of (In,Ga)(As,N)/

(Al,Ga)As MQWs. These samples were grown on semi-insulating (SI) GaAs substrates by molecular-beam epitaxy (MBE) as described in Ref. 7. Each MQW consists of 50 periods with a nitrogen content $N_N \leqslant 4\%$. The wells of the MQWs are doped with Si, where the Si concentration n_{Si} increases from $n_{Si}=2\times10^{18}$ cm^{-3} for $N_N \leqslant 0.1\%$ to $n_{Si}=5\times10^{18}$ cm^{-3} for $N_N \geqslant 2\%$ in order to compensate for the increasing electrical passivation of the Si donors with increasing N_N. The concentration n and mobility μ of the free carriers were determined by Hall measurements, while the spatial distribution of the free carriers in the MQWs were verified by capacitance-voltage (C-V) measurements.

The experimentally determined carrier concentrations at room temperature agree with the nominal values. At $T=300$ K, the Hall mobility decreases from about $\mu=1700$ cm^2 (Vs)$^{-1}$ for samples without N to about 400 cm^2 (Vs)$^{-1}$ for MQWs with 0.1% N and decreases even further to values between 200 and 100 cm^2 (Vs)$^{-1}$ for samples with $N_N \geqslant 0.8\%$. This dependence of μ on N_N at $T=300$ K is interpreted in the following way. In samples without N, scattering of electrons on longitudinal optical phonons as well as on ionized impurities is dominating, while with increasing N content electrons are more and more scattered by N-related defects including alloy scattering and potential fluctuations due to N clusters.[7–10] With decreasing temperature down to about 77 K, the mobility of the N-containing samples remains almost constant (predominantly defect scattering), whereas for 10 K$<T<$77 K weak localization determines the mobility. Below 10 K, hopping conduction prevails.[7–10]

We have studied two sets of MQWs. In the first set (MQWs I), the wells also contain In with $N_{In} \approx 3N_N$ in order to compensate for the strain due to the N atoms. The well width d_w was chosen to be 6 nm. The barriers consist of $Al_{0.33}Ga_{0.67}As$ with a thickness $d_b=10$ nm. Measurements on different MQWs have shown that an In content of $N_{In} \leqslant 12\%$ in the wells does not substantially change the ISA spectra. Therefore, in the second set of samples (MQWs II), the wells are grown without In. The well width d_w was chosen to be 3 nm, and the barriers consist of $Al_{0.42}Ga_{0.58}As$ with a thickness $d_b=10$ nm. All samples were analyzed by x-ray diffraction, which indicates that the actual length of the periods, the N content of the wells, and the composition of the barriers agree well with the nominal data. In the following, we will focus on as-grown samples, because a rapid thermal annealing of the MQWs for temperatures below 850 °C, which usually improves the interband emission characteristics,[11] does not significantly change the ISA spectra.

The ISA spectra were measured by two methods. First, a single transmission of polarized light at oblique incidence (angle of incidence 60°) through plane parallel samples was detected. Second, in order to considerably improve the signal-to-noise ratio, the transmission was studied through waveguide-shaped samples (45° facets and 7 internal reflections). Measurements were carried out at room temperature as well as for selected samples at $T=77$ K using a Fourier-transform spectrometer (Bruker IFS 66v). The spectra recorded for p-polarized light (T_p) were normalized to the ones for s-polarized light (T_s). The obtained T_p/T_s spectra of the samples were additionally normalized to the $(T_p/T_s)_0$ spectrum of a SI-GaAs reference substrate in order to remove any effects due to the prepolarization of the Fourier-transform spectrometer as well as the SI-GaAs substrate. For the detection of the weak and very broad absorption bands, the measurements were carried out for different sample and polarizer orientations (vertical and horizontal), and the final spectra were obtained by averaging over all T_p/T_s spectra.

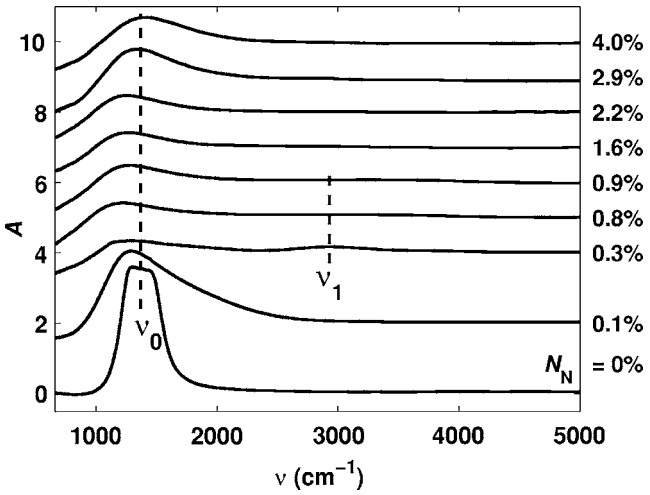

FIG. 1. Absorbance spectra of (In,Ga)(As,N)/(Al,Ga)As MQWs with $d_w=6$ nm and $Al_{0.33}Ga_{0.67}As$ barriers (MQWs I) at room temperature for increasing N_N from bottom to top as indicated on the right-hand side. The main ISA band and the high-frequency absorption feature are indicated by ν_0 and ν_1, respectively. The dashed lines are guides to the eye. The spectra are vertically shifted for clarity. The increment is 2 for the two MQWs with the lowest N content ($N_N=0.1\%$ and 0.3%), whereas it is 1 for MQWs with higher N content.

III. INTERSUBBAND ABSORPTION SPECTRA OF MQWS

For samples without nitrogen, the transmission spectra for a single light pass exhibit a minimum due to ISA, where the transmittance $T=(T_p/T_s)/(T_p/T_s)_0$ decreases to about 88%. The full width at half minimum (FWHM) is about 150 cm^{-1}. For the MQWs with $N_N>0.1\%$, the ISA minimum becomes much less pronounced (its value decreases to 98%). At the same time, the minimum becomes much broader (FWHM $\approx$400 cm^{-1}), i.e., the absorption becomes very weak. Therefore, we will only discuss ISA spectra of (In,Ga)$\times$(As,N)/(Al,Ga)As and Ga(As,N)/(Al,Ga)As MQWs measured using the much more sensitive internal reflection method on waveguide-shaped samples. For presenting these spectra, we use the absorbance as given by $A=-\ln(T_p/T_s)$ corrected by the background signal given by $+\ln(T_p/T_s)_0$.

Figure 1 shows ISA spectra of the MQWs I for increasing N_N recorded at 300 K. The spectrum of the sample without N displays a pronounced absorption band at $\nu_0=(1365\pm10)$ cm^{-1}. In the spectrum of the sample with $N_N \approx 0.1\%$ (nominally 0.08%), the absorption band at ν_0 is already somewhat redshifted and exhibits on the high-

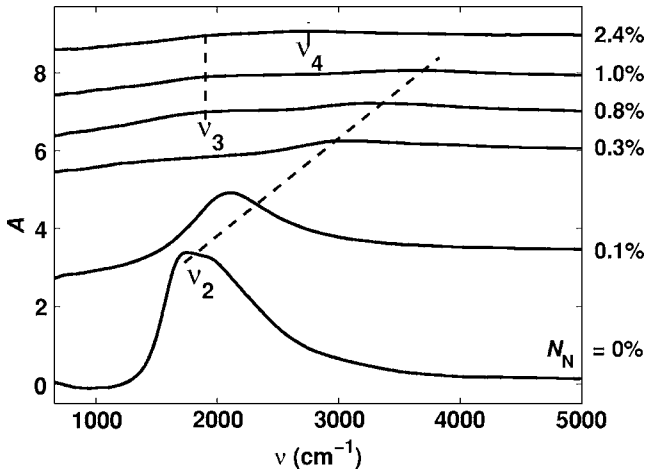

FIG. 2. Absorbance spectra of Ga(As,N)/(Al,Ga)As MQWs with d_w=3 nm and $Al_{0.42}Ga_{0.58}As$ barriers (MQWs II) at room temperature for increasing N_N from bottom to top as indicated on the right-hand side. The main ISA band (low-frequency absorption features) is indicated by ν_2 (ν_3 and ν_4). The dashed lines are guides to the eye. The spectra are vertically shifted for clarity. The offsets ΔA are 3.5 for N_N=0.1%, 6 for 0.3%, 7 for 0.8%, 8 for 1%, and 9 for 2.4%.

frequency side a strong asymmetric broadening. This trend continues in the ISA spectrum for the sample with N_N =0.3%, which shows besides the very broad band at ν_0 =(1212±10) cm^{-1} a second absorption band at ν_1 =(2930±30) cm^{-1}, where the intensity of both absorption bands is already remarkably reduced with respect to the ISA band of the MQW without N. With increasing N_N up to 1.6%, the small decrease of ν_0 continues, and the spectral feature at ν_1 disappears due to broadening effects. Finally, for the samples with $N_N \geq 2.2\%$, the wave number ν_0 slightly increases with increasing N_N and reaches the value ν_0 =(1405±10) cm^{-1} for N_N=4%.

The ISA spectra of the MQWs II are shown in Fig. 2 for increasing N content recorded at 300 K. The spectrum of the sample without N shows a pronounced absorption band at ν_2=(1820±15) cm^{-1}. However, in contrast to the ISA spectrum of the MQW I with N_N=0, the main ISA band for the MQW II with N_N=0 exhibits already a strong asymmetric broadening on the high-frequency side. For the spectrum of the sample with $N_N \approx 0.1\%$, the main ISA band is clearly blueshifted, and the asymmetry on the high-frequency side persists. With a further increase of N_N, the intensity of the ISA bands remarkably decreases, and on the low-frequency side of the band at ν_2 a weak very broad absorption feature appears at $\nu_3 \approx 1900$ cm^{-1}. Finally, in the spectrum of the sample with N_N=2.4%, the main ISA band disappears, the low-frequency feature remains, and a new feature appears at about 2750 cm^{-1}.

For 77 K, the dependence of the ISA spectra on the nitrogen content is almost the same as for 300 K. We believe that this observation can be explained as follows. First, due to the high concentration of free carriers in the samples, the electron gas is nearly degenerate. Therefore, the electron distribution in the occupied first subband as well as in the almost unoccupied second subband hardly changes with decreasing temperature down to 77 K. Second, as discussed in Sec. II, the strong scattering of the electrons on N-related defects for the N-containing MQWs does not change for temperatures between 77 and 300 K. Therefore, the large FWHM of the ISA bands remains with decreasing temperature down to 77 K.

IV. THREE-BAND k·p HAMILTONIAN FOR Ga(As,N)/(Al,Ga)As MQWS

The small redshift observed in MQWs I and II with increasing N content is the essential experimental result. This is in contrast to an expected blueshift, if the influence of N is only taken into account on the band offset. Therefore, we will focus on analyzing the IST energies as a function of N_N. The second important feature of all ISA bands of the MQWs with $N_N > 0.2\%$ is the remarkable reduction of their intensity and the strong increase of their FWHM. We believe that these features are predominantly caused by the strong scattering of electrons on N-related defects (cf. Sec. II) and are not determined by the oscillator strengths of these ISTs. Therefore, a quantitative description of the line shape requires a scattering theory for the free carriers on N-related defects, which is beyond the scope of this investigation.

While the MQWs I contain indium in the wells, this is not the case for the MQWs II. However, for the MQW I with the largest In content, the change in the wave number ν_{12} of the IST from the ground ($|1\rangle$) to the first excited subband ($|2\rangle$) is smaller than the uncertainty of the experimental value ν_0. Therefore, in the following, we will ignore the influence of indium on the conduction band structure, and the energies of the subbands are only calculated for Ga(As,N)/(Al,Ga)As MQWs within a three-band $\mathbf{k}\cdot\mathbf{p}$ approximation. This three-band $\mathbf{k}\cdot\mathbf{p}$ model takes into account the effect of N on the conduction band structure and the nonparabolicity in the Ga(As,N) wells as well as the (Al,Ga)As barriers. The conduction band structure of each individual layer within a heterostructure is described by the tight-binding Hamiltonian[2,3]

$$\hat{H} = \begin{pmatrix} E_N + \alpha_N k_z^2 & V_{NC} - \alpha_{NC} k_z^2 & P_N k_z \\ V_{NC} - \alpha_{NC} k_z^2 & E_C - \alpha_C k_z^2 & P_1 k_z \\ P_N k_z & P_1 k_z & E_V + \alpha_V k_z^2 \end{pmatrix}, \tag{1}$$

where k_z denotes the component of the wave vector along the growth direction of the MQWs. E_N, E_C, and E_V are the energies of the original states, taking into account that their energies are slightly changed due to the N incorporation (disorder and band tails, formation of clusters, partial breakdown of $\mathbf{k}$-selection rules, etc.). The coefficients α are related to the effective masses of the different states. For the localized N state, a very flat dispersion is used, which corresponds to a very large effective mass.[2] The coupling between the original states is described by the off-diagonal coefficients V_{NC}, P_N, and P_1. The coupling between the N state and the conduction (valence) band edge disappears for N_N=0 because $V_{NC} \propto \sqrt{N_N}$($P_N \propto \sqrt{N_N}$) is assumed.[2] The constant P_1 accounts for the coupling between the conduction and valence band edges

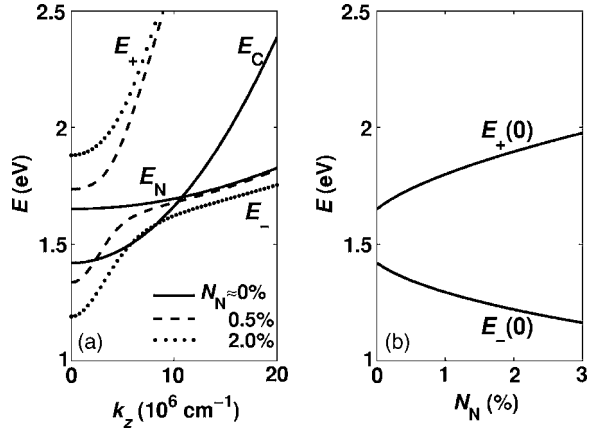

FIG. 3. Anticrossing behavior of the mixed conduction band branches E_+ and E_- for bulk Ga(As,N) as a function of (a) k_z according to Eq. (1) for N_N=0, 0.5, and 2% and (b) N_N according to Eq. (2) for k_z=0.

in GaAs at Γand is independent of N_N. The (Al,Ga)As barriers are also described by the Hamiltonian in Eq. (1), with all N-depending terms as well as E_N being set to zero. The parameters used in the calculation are given in Ref. 12.

For bulk Ga(As,N) at k_z=0, the Hamiltonian in Eq. (1) has three solutions, E_+, E_-, and E_3

$$E_{\pm}(N_N,\ k_z=0)=\frac{E_N+E_C}{2}\pm\frac{1}{2}\sqrt{(E_N-E_C)^2+4V_{NC}^2(N_N)}$$
$$\text{and}\quad E_3=E_V. \tag{2}$$

Figure 3(a) shows the anticrossing behavior of the mixed conduction band branches E_+ and E_- versus k_z in bulk Ga(As,N) for N_N=0, 0.5, and 1% according to Eq. (2), while in Fig. 3(b) the values E_+ and E_- are plotted versus N_N. The energies E_+ and E_- describe the pseudogap between the conduction branches for a given N_N at k_z=0 as already described within the two-band model.[1,2]

In order to calculate the eigenstates for the heterostructure, we switch to real space by replacing in Eq. (1) the momentum k_z by its quantum-mechanical operator $(1/i)\partial/\partial z$.[13] By assuming periodic boundary conditions for the whole structure (such as in a MQW or superlattice), we can apply a discrete Fourier transformation. The wave functions for the subbands of the complete structure are then given by

$$\Psi_{k_z,v}(z)=\frac{1}{d}e^{ik_zd}\sum_{n,j}c_{k_zv,nj}\exp\left(\frac{2\pi ij}{d}z\right)|\mathbf{u}_n\rangle, \tag{3}$$

where d denotes the period of the MQW or superlattice, v the subband index, j the Fourier expansion index, and $\mathbf{u}_n$ (n=1,2,3) the base vectors of the three-band $\mathbf{k}\cdot\mathbf{p}$ model. In this basis, the eigenvalue equation for the heterostructure can be written as

$$\sum_{n',j'}H_{nj,n'j'}(k_z)c_{k_zv,n'j'}=E_{k_zv}c_{k_zv,nj}, \tag{4}$$

with the matrix elements denoted by

$$H_{nj,n'j'}(k_z)=\frac{1}{d}\int_0^d dz\exp\left(\frac{-2\pi i\bar{j}}{d}z\right)\times\langle u_n|H(z)|u_{n'}\rangle\exp\left(\frac{-2\pi i\bar{j}'}{d}z\right), \tag{5}$$

where $\bar{j}=j+q_z$, $-\frac{1}{2}\leqslant q_z\leqslant 1/2$, and $k_z=2\pi q_z/d$. The matrix elements $\langle u_n|H(z)|u_{n'}\rangle$ of the Hamiltonian that describes the MQW structure are analytically calculated assuming that the confinement potentials are constant within each layer. Putting everything together, the eigenstates of the complete MQW structure are calculated from the eigenvalue equation of a Hermitian matrix

$$\hat{H}_{jj'}=\sum_{m=0}^{n}\begin{pmatrix} E_{N_m}+\alpha_{N_m}\left(\frac{2\pi}{d}\right)^2j'^2 & V_{NCm}-\alpha_{NCm}\left(\frac{2\pi}{d}\right)^2j'^2 & P_{N_m}\frac{2\pi}{d}j' \\ V_{NCm}-\alpha_{NCm}\left(\frac{2\pi}{d}\right)^2j'^2 & E_{C_m}-\alpha_C\left(\frac{2\pi}{d}\right)^2j'^2 & P_1\frac{2\pi}{d}j' \\ P_{N_m}\frac{2\pi}{d}j' & P_1\frac{2\pi}{d}j' & E_{V_m}+\alpha_V\left(\frac{2\pi}{d}\right)^2j'^2 \end{pmatrix}\times g_m(j,j'), \tag{6}$$

where

$$g_m(j,j')=\begin{cases}(d_m-d_{m-1})/d & \text{for}\quad j=j',\\ \{1/[2\pi(j'-j)]\}\{\exp[2\pi(j'-j)d_m/d]-\exp[2\pi(j'-j)d_{m-1}/d]\} & \text{for}\quad j\neq j'.\end{cases} \tag{7}$$

In deriving this form for the matrix, the modified Galerkin method[14] has been applied. The solution of the eigenvalue problem is straightforward. In the numerical procedure, we approximate the solution by only taking into account a finite number of Fourier coefficients $|j|$ and $|j'|\leqslant 300=j_{max}$ so that convergence is achieved. In Eq. (7), d_m denotes the z coor-

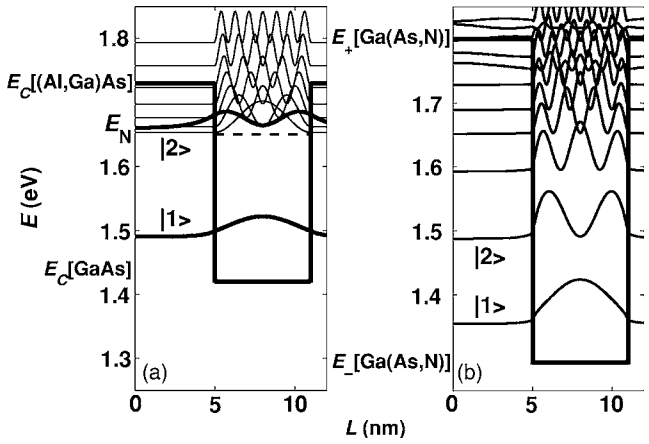

FIG. 4. Conduction subband structure for Ga(As,N)/(Al,Ga)As MQWs with $d_w=6$ nm and $Al_{0.33}Ga_{0.67}As$ barriers (MQWs Ib). (a) $|\Psi|^2$ calculated for small N content. The thick solid lines represent the original bound states $|1\rangle$ and $|2\rangle$ in the quantum well for $N_N=0$. The thin solid lines indicate the N-like states, which are caused by the localized N state at E_N for very low N content. (b) $|\Psi|^2$ for $N_N=1\%$. The lines represent $|\Psi|^2$ of the mixed subbands formed due to the coupling between the original bound and the N-like states in the quantum well.

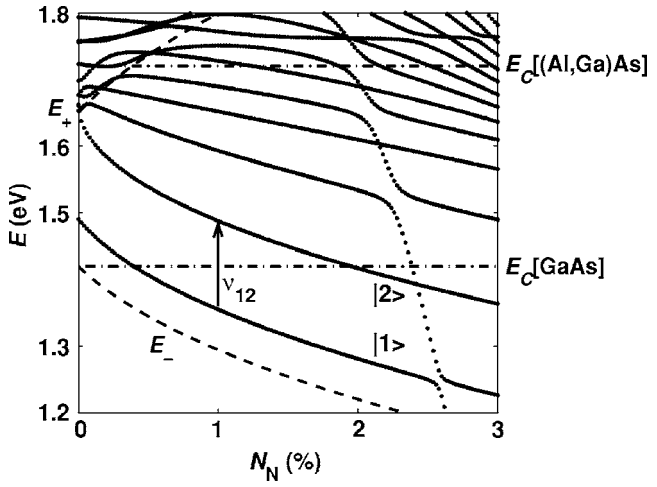

FIG. 5. Calculated energies for the subbands of Ga(As,N)/(Al,Ga)As MQWs with $d_w=6$ nm and $Al_{0.33}Ga_{0.67}As$ barriers (MQWs Ib) vs N content (solid and dotted lines). The dashed-dotted lines represent the conduction band edges of GaAs and $Al_{0.33}Ga_{0.67}As$, while the dashed lines indicate the energies $E_+(N_N)$ and $E_-(N_N)$ for the two conduction band branches of Ga(As,N) [Eq. (2)]. The IST from the ground $|1\rangle$ into the first excited subband $|2\rangle$ is indicated by ν_{12}.

dinate of the mth interface along the growth direction, where $d_0=0$ was assumed so that $d_n=d$. For bulk materials (a single layer), the Hamiltonian in Eq. (6) becomes block diagonal with 3×3 submatrices, because $g_m(j,j')=\delta_{jj'}$, and the eigenvalues of this block matrix describe the band structure.

V. COMPARISON OF THE CALCULATED INTERSUBBAND TRANSITION ENERGIES WITH EXPERIMENTAL DATA FOR Ga(As,N)/(Al,Ga)As MQWS

In this section, we apply the solution of the eigenvalue problem of the matrix given in Eq. (6) to the conduction band structure of Ga(As,N)/(Al,Ga)As MQWs. At first, we discuss the data, which were calculated for MQWs with $d_w=6$ nm and $Al_{0.33}Ga_{0.67}As$ barriers. These heterostructures are labeled MQWs Ib, since they have the same layer structure as the experimentally investigated samples MQWs I, but do not contain In in the wells. Figure 4 shows the calculated band structure for two MQWs Ib. For the MQW Ib without any nitrogen [cf. Fig. 4(a)], the quantum well contains two bound states $|1\rangle$ and $|2\rangle$, which are indicated as thick solid lines. For this MQW, the discontinuity of the conduction band is determined by E_C[GaAs] and $E_C[Al_{0.33}Ga_{0.67}As]$. In Ga(As,N) with very low N content, a localized N state is formed at $E_N=1.65$ eV (Ref. 1) indicated in Fig. 4 by the dashed line and included in Eq. (6) by the E_{N_m}-dependent diagonal element. An important consequence of Eq. (6) is that due to the QW confinement the *localized N state creates an additional set of N-like states in each quantum well above* E_N, which are indicated in Fig. 4(a) as thin solid lines. Due to the large effective mass of the N state and the small energy difference between the barrier and E_N, the energy separation between neighboring N-like levels is smaller than the one between the original quantum well states $|1\rangle$ and $|2\rangle$. For $N_N>0.3\%$, the energy of the bottom of the quantum well shifts according to Eq. (2) from E_C[GaAs] to $E_-(N_N)$, whereas the energy of the top of the quantum well increases from $E_C[(Al,Ga)As]$ to $E_+(N_N)$. While in Ref. 6 only the increase in the band offset was taken into account in the calculation of the subband energies for (In,Ga)(As,N)/GaAs MQWs, the three-band $\mathbf{k}\cdot\mathbf{p}$ model in Sec. IV explicitly includes the nonparabolicity and the coupling of the states at E_C and E_V with the ones at E_N, which is described in Eq. (6) by the N-dependent off-diagonal elements. For $N_N=0$, this coupling disappears. However, for $N_N>0$, these off-diagonal terms cannot be neglected anymore. Due to this coupling, *the N-like states in the quantum wells mix with the original ones* already present for $N_N=0$. $|\Psi|^2$ of these mixed subbands is shown by the lines in Fig. 4(b) for $N_N=1\%$.

In Fig. 5, the calculated subband energies $E_i(N_N)$, where $i=1,2,\ldots,3(2j_{max}+1)$ denotes the index of the newly formed mixed subband, are plotted as solid and dotted lines for the MQWs Ib. For a better overview, the high-frequency as well as the low-frequency conduction band branches of Ga(As,N) (E_- and E_+, respectively) are also included in the figure as dashed lines, while the original energies of the bottom and the top of the quantum well (E_C[GaAs] and $E_C[(Al_{0.33}Ga_{0.67})As]$, respectively) are indicated as dashed-dotted lines. The newly formed mixed bound states exhibit alternating anticrossings and crossings with increasing energy as expected from the symmetry of the subbands (cf. Fig. 5). However, the anticrossing behavior is not the subject of the present study. Figure 5 clearly shows the formation of the mixed subbands as well as their redshift with increasing N_N.

The calculated wave number $\nu_{12}(N_N)=E_2(N_N)-E_1(N_N)$ for the IST from the ground $|1\rangle$ into the first excited subband $|2\rangle$ is plotted in Fig. 6 as a solid line. The redshift of all newly formed mixed subbands causes the important effect

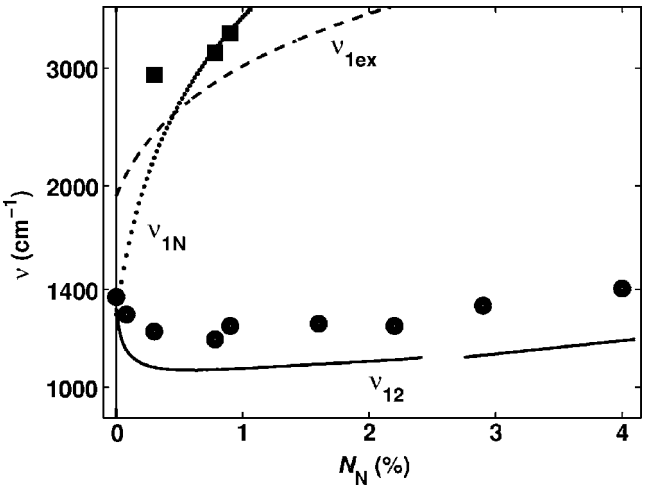

FIG. 6. Semilogarithmic plot of the measured (symbols) and calculated (lines) wave numbers for ISTs in Ga(As,N)/(Al,Ga)As MQWs with d_w=6 nm and $Al_{0.33}Ga_{0.67}As$ barriers (MQWs I and Ib) vs N content. The wave number ν_0 for the main absorption band (ν_1 for the high-frequency absorption feature) in the ISA spectra of the MQWs I shown in Fig. 1 is marked as dots (squares). The solid line indicates the calculated wave number ν_{12} for the IST from the ground into the first excited subband. The dashed (dotted) line denotes the IST from the ground state into the continuum above the $Al_{0.33}Ga_{0.76}As$ barriers [above the upper pseudogap at $E_+(N_N)$ of the Ga(As,N) wells]. Note that the gaps in the solid line reflects the minigap in the conduction subband structure of Fig. 5.

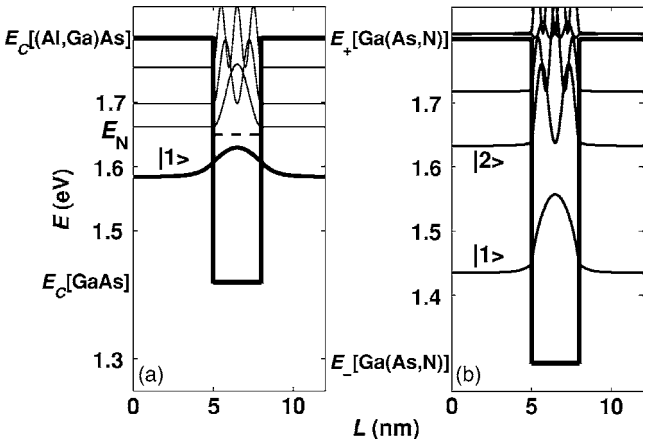

FIG. 7. Conduction subband structure for Ga(As,N)/(Al,Ga)As MQWs with d_w=3 nm and $Al_{0.42}Ga_{0.58}As$ barriers (MQW II). (a) $|\Psi|^2$ calculated for small N content. The thick solid line represents the original bound state $|1\rangle$ in the quantum well, which is already present for N_N=0. The thin solid lines indicate the N-like states, which are caused by the localized N state at E_N for very low N content. (b) $|\Psi|^2$ calculated for N_N=1%. The lines represent $|\Psi|^2$ of the mixed subbands formed due to the coupling between the original bound and the N-like states in the quantum well.

that the IST energy ν_{12} decreases very rapidly with increasing nitrogen content for $N_N \leqslant 0.3\%$. With a further increase of N_N, the value of ν_{12} reaches a minimum at $N_N \approx 0.5\%$ and then slightly increases. In Fig. 6, the measured wave numbers ν_0 for the main ISA band of the MQWs I are marked as dots. These data were taken from the maxima of the main absorption band in the ISA spectra shown in Fig. 1. Figure 6 shows that the calculated values $\nu_{12}(N_N)$ for the MQWs Ib are in good agreement with the measured N dependence of $\nu_0(N_N)$ for the MQWs I. Therefore, we attribute the main absorption band in the ISA spectra of the MQWs I to the IST from the ground $|1\rangle$ into the first excited subband $|2\rangle[\nu_0 = \nu_{12}(N_N)]$. Note that deviations between the calculated and the measured energies may occur for several reasons. First, electron-electron interactions, in particular the depolarization shift, are neglected in the calculations. Second, the coupling between plasmons and ISTs is not taken into account. Third, the influence of In on the conduction band structure is not included as mentioned above. Fourth, due to the large width of the ISA minima, the uncertainty of the ν_0 values is rather large. Furthermore, the strong asymmetry of the absorption minima may result in some systematic deviations. Fifth, due to the strong free-carrier scattering as indicated by the broad minima in the ISA spectra in Figs. 1 and 2, the coupling between the N-like and the original quantum states in the wells may by reduced, which causes an additional frequency shift for the intersubband excitations, which is not taken into account in this study. Such damping effects reduce the anticrossing of any coupled elementary excitations in a solid.[15]

In the MQWs Ib containing N, several mixed subbands are formed as discussed above and shown in Figs. 4(b) and 5. Therefore, we also expect transitions from the ground state $|1\rangle$ into higher subbands than the second one, but with a decreasing oscillator strength with increasing subband separation. We assume that these transitions cause the strong asymmetric broadening on the high-frequency side of the main ISA band at ν_0 shown in Fig. 1. Furthermore, for sufficiently high N concentration ($N_N \approx 0.3\%$), the density of the higher subband levels becomes large enough in order to also enable ISTs from the ground state $|1\rangle$ into the continuum above the barrier $E_C[Al_{0.33}Ga_{0.67}As]$, which are denoted in Fig. 6 by ν_{1ex} (dashed line). With a further increase of N_N beyond 0.3%, the high-frequency edge $E_+(N_N)$ of the quasigap [Eq. (2)] exceeds the energy of the barriers $E_C[(Al,Ga)As]$ and extends into the quasicontinuum above the barrier. This may cause ISTs from the subband $|1\rangle$ into states with an energy $E \geqslant E_+[Ga(As,N)]$. In Fig. 6, these transitions are denoted by ν_{1N} (dotted line). From a comparison of the dashed and dotted lines with the high-frequency absorption feature at ν_1 for the MQWs I with $0.3\% \leqslant N_N \leqslant 1\%$ as taken from Fig. 1 (squares in Fig. 6), we conclude that the ISA band at ν_1 is caused by a bound-to-continuum transition.

For a further demonstration of the formation of new subbands in the wells, we have investigated ISTs in Ga(As,N)/(Al,Ga)As MQWs with d_w=3 nm and $Al_{0.42}Ga_{0.58}As$ barriers (MQWs II). The corresponding ISA spectra are shown in Fig. 2. Due to the small width of the quantum wells, the MQWs II exhibit for N_N=0 only one bound state $|1\rangle$ in the well as shown by the thick solid line in Fig. 7(a). Therefore, the MQWs II should exhibit only a bound-to-continuum IST, even if the energy of the bottom (top) of the quantum well decreases (increases) with increasing N_N according to Eq. (2). However, within the three-band $\mathbf{k}\cdot\mathbf{p}$ model of Sec. IV, additional N-like states are created in

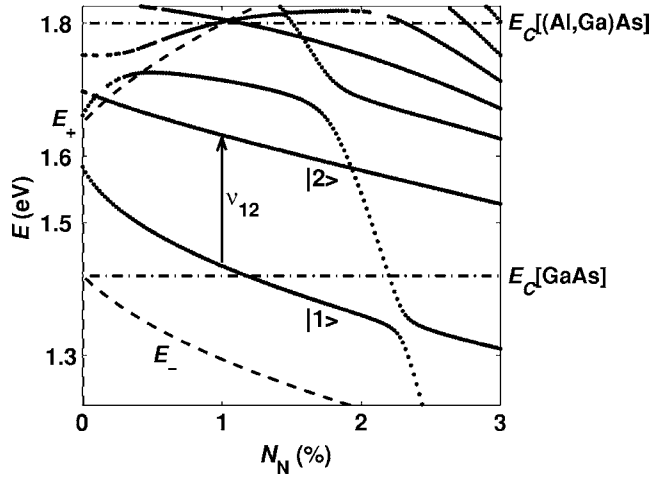

FIG. 8. Calculated energies for the subbands of Ga(As,N)/(Al,Ga)As MQWs with $d_w=3$ nm and $Al_{0.42}Ga_{0.58}As$ barriers (MQWs II) vs N content (solid and dotted lines). The dashed-dotted lines represent the conduction band edges for GaAs and $Al_{0.42}Ga_{0.58}As$, while the dashed lines indicate the energies $E_+(N_N)$ and $E_-(N_N)$ for the two conduction band branches of Ga(As,N) [Eq. (2)]. The IST from the ground $|1\rangle$ into the first excited subband $|2\rangle$ is indicated by ν_{12}.

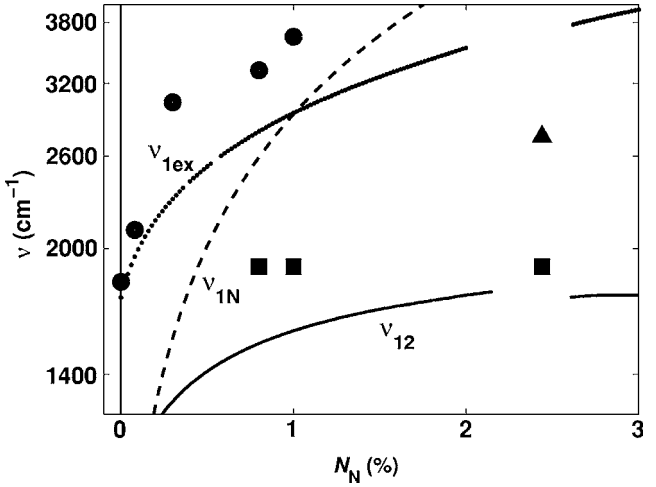

FIG. 9. Semilogarithmic plot of the measured (symbols) and calculated (lines) wave numbers for ISTs in Ga(As,N)/(Al,Ga)As MQWs with $d_w=3$ nm and $Al_{0.42}Ga_{0.58}As$ barriers (MQWs II) vs N content. The wave number ν_2 for the main absorption band (ν_3 for the low-frequency absorption feature) in the ISA spectra of the MQWs II shown in Fig. 2 is marked as dots (squares), whereas the triangle indicates an additional absorption feature. The solid line indicates the calculated wave number ν_{12} for the IST from the ground into the first excited subband. The dashed (dotted) line denotes the IST from the ground state into the continuum above the $Al_{0.42}Ga_{0.58}As$ barriers [above the upper pseudogap at $E_+(N_N)$ of the Ga(As,N) wells]. Note that the gaps in the lines reflect the minigaps in the conduction subband structure of Fig. 8.

the wells, which are shown for small values of N_N in Fig. 7(a) as thin solid lines. The coupling of these states with the original bound state in the well results in the formation of several new mixed subbands with the corresponding $|\Psi|^2$ shown in Fig. 7(b) for the MQW II with $N_N=1\%$. The energies of these new mixed subbands for the MQWs II are plotted in Fig. 8 as a function of N_N as solid and dotted lines. Figure 8 shows that within the three-band $\mathbf{k}\cdot\mathbf{p}$ model more than one bound state is present in the wells of the MQWs II for $N_N \geqslant 0.3\%$. Therefore, we expect also a bound-to-bound IST $|1\rangle \rightarrow |2\rangle$ in the MQWs II, if the N concentration and, therewith, the density of states of the new mixed subbands is sufficiently large.

In Fig. 9, the calculated (measured) energies for different ISTs in the MQWs II are shown versus N_N as lines (symbols). At first, we analyze the main ISA band at ν_2, which is indicated in Fig. 9 by the dots. The dotted line in Fig. 9 represents the calculated energies for the IST from the ground state $|1\rangle$ into the quasicontinuum above the $Al_{0.42}Ga_{0.58}As$ barriers, which is denoted by ν_{1ex}. For the MQW II with $N_N=0$, the calculated value of ν_{1ex} agrees exactly with the measured one indicating that the main ISA band is due to such a bound-to-continuum transition above the (Al,Ga)As barriers. This assignment is also supported by the strong asymmetric broadening on the high-frequency side of the main ISA band (cf. Fig. 2), which is typical for such a transition.[16,17] With increasing N_N, the energy of the bottom of the quantum well decreases according to $E_-(N_N)$ resulting in an increasing wave number ν_{1ex} for this IST. For $N_N \geqslant 1\%$, the energy $E_+(N_N)$ of the upper conduction band branch exceeds the one of the barriers $E_C[Al_{0.42}Ga_{0.58}As]$. Therefore, the IST now occurs from the ground state $|1\rangle$ into the continuum above the pseudogap at $E_+(N_N)$ of the Ga(As,N) wells. In Fig. 9, this IST is denoted by ν_{1N} (dashed line). A comparison of the measured wave number ν_2 of the main ISA band (dots) with the calculated values ν_{1N} for the MQWs II suggests that the main ISA band at ν_2 is caused by such a bound-to-continuum IST for $N_N \geqslant 1\%$.

In the following, we analyze the wave numbers ν_3 of the low-frequency spectral feature in the ISA spectra of the MQWs II with $N_N \geqslant 0.8\%$ (cf. Fig. 2). The values of ν_3 are marked in Fig. 9 by squares. The appearance of this spectral feature below the bound-to-continuum transition at ν_2 must be due by a second bound state in the quantum well, which is predicted by our three-band BAC model as shown in Fig. 8 for $N_N > 0.3\%$. The calculated wave number $\nu_{12}(N_N)$ for the $|1\rangle \rightarrow |2\rangle$ IST for the MQWs II is indicated as the solid line in Fig. 9. This plot shows that the additional low-frequency absorption feature at ν_3 measured for the MQWs II with $N_N=2.4\%$ approaches the calculated values ν_{12} [$\nu_3 \approx \nu_{12}(N_N)$]. Therefore, we assume that the ISA band at ν_3 is an additional confirmation that the model presented in Sec. IV actually describes the influence of N on bound-to-bound as well as bound-to-continuum ISTs in Ga(As,N)/(Al,Ga)As MQWs. The deviation of the wave numbers of the spectral feature at ν_3 for the MQWs with $N_N \leqslant 1\%$ from the calculated ν_{12} values (solid line) may be due to a spectral overlap of the low-frequency ISA spectral feature at ν_3 with the strong main ISA band of the bound-to-continuum IST at ν_2. Finally, we note that the wave number of the additional absorption feature for the MQW II with $N_N=2.4\%$ indicated by the triangle in Fig. 9 nearly agrees with the calculated wave number for the IST from the first into the fourth subband.

VI. SUMMARY AND CONCLUSIONS

The effect of the quantum well confinement on a localized N state creates a number of N-like states in each quantum well of (In,Ga)(As,N)/(Al,Ga)As MQWs. Due to the coupling of these N-like states with the original well states, new mixed subbands are formed in the conduction band structure of the MQWs. This effect essentially modifies the energies of the bound-to-bound as well as bound-to-continuum ISTs. The intensity and the width of the ISA spectra are clearly affected by the strong scattering of electrons on N-related defects. We conclude that this scattering probably prevents lasing in N-containing GaAs-based quantum-cascade lasers. In addition, the strong modification of the conduction band structure in Ga(As,N)/(Al,Ga)As quantum-cascade structures has to be taken into account for the design of N-containing GaAs-based quantum-cascade lasers.

ACKNOWLEDGMENTS

The authors would like to thank L. Schrottke for valuable discussions and H. v. Kiedrowski for the preparation of the waveguide-shaped samples.

*Electronic address: giehler@pdi-berlin.de

[1] W. Shan, W. Walukiewicz, J. W. Ager III, E. E. Haller, J. F. Geisz, D. J. Friedman, J. M. Olson, and S. R. Kurtz, Phys. Rev. Lett. **82**, 1221 (1999).

[2] E. P. O'Reilly and A. Lindsay, Phys. Status Solidi B **216**, 131 (1999).

[3] E. P. O'Reilly, A. Lindsay, S. Tomic, and M. Kamal-Saadi, Semicond. Sci. Technol. **17**, 870 (2002).

[4] See, e.g., Semicond. Sci. Technol. **17**(8) 2002, topical issue, edited by J. W. Ager III and W. Walukiewicz, and references therein.

[5] A. Guzmán, E. Luna, J. Miguel-Sánchez, E. Calleja, and E. Muñoz, Infrared Phys. Technol. **44**, 377 (2003).

[6] J.-Y. Duboz, J. A. Gupta, M. Byloss, G. C. Aers, H. C. Liu, and Z. R. Wasilewski, Appl. Phys. Lett. **81**, 1836 (2002); J.-Y. Duboz, J. A. Gupta, Z. R. Wasilewski, J. Ramsey, R. L. Williams, G. C. Aers, B. J. Riel, and G. I. Sproule, Phys. Rev. B **66**, 085313 (2002).

[7] R. Hey, Y.-J. Han, M. Giehler, M. Ramsteiner, H. T. Grahn, and K. H. Ploog, J. Cryst. Growth **278**, 219 (2005).

[8] J. F. Geisz and D. J. Friedman, Semicond. Sci. Technol. **17**, 769 (2002).

[9] R. Mouillet, L.-A. de Vaulchier, E. Deleporte, Y. Guldner, L. Travers, and J.-C. Harmand, Solid State Commun. **126**, 333 (2003).

[10] A. Hashimoto, T. Yamaguchi, T. Suzuki, and A. Yamamoto, J. Cryst. Growth **278**, 532 (2005).

[11] G. Mussler, L. Däweritz, K. H. Ploog, J. W. Tomm, and V. Talalaev, Appl. Phys. Lett. **83**, 1343 (2003).

[12] In the calculation, the following parameters were used for the uncoupled states in the wells: $E_N = E_{N_0} - (\gamma - \kappa)\tilde{N}_N$, $E_C = E_{C_0} - (\alpha - \kappa)\tilde{N}_N$, and $E_V = E_{V_0} + \kappa\tilde{N}_N$, where $E_{C_0} = 1.42$ eV, $E_{V_0} = -0.02$ eV, $E_{N_0} = 1.65$ eV, $\alpha = 1.55$ eV, $\gamma = 3.89$ eV, $\kappa = 3.88$ eV, and $\tilde{N}_N = N_N$ (in %)/100 (Ref. 2). Coupling coefficients: $V_{NC} = \beta\sqrt{\tilde{N}_N}$, where $\beta = -2.3$ eV ($P_N = \tilde{\beta}\sqrt{\tilde{N}_N}$, with $\tilde{\beta} = -0.983$ eV Å). $P_1 = 9.753$ eV Å (Refs. 2 and 3). Dispersion parameters: $\alpha_N = (1.099 - 885\tilde{N}_N^2)$ eV Å^2, $\alpha_C = 6.047$ eV Å^2, $\alpha_V = 1.683$ eV Å^2, and $\alpha_{NC} = -3.112$ eV Å^2 (Ref. 2). (Al,Ga)As barrier parameters: $E_N = V_{NC} = P_N = 0$, $P_1 = 9.753$ eV Å. MQWs I: $E_{C_0} = 1.73$ eV and $E_{V_0} = -0.17$ eV, MQWs II: $E_{C_0} = 1.8$ eV and $E_{V_0} = -0.20$ eV.

[13] D. Gershoni, C. H. Henry, and G. A. Baraff, IEEE J. Quantum Electron. **29**, 2433 (1993).

[14] G. B. Morrison, S. C. Woodworth, H. Wang, and D. T. Cassidy, IEEE J. Quantum Electron. **40**, 222 (2004).

[15] M. Giehler and E. Jahne, Phys. Status Solidi B **73**, 503 (1976).

[16] B. F. Levine, K. K. Choi, C. G. Bethea, J. Walker, and R. J. Malik, Appl. Phys. Lett. **50**, 1092 (1987).

[17] Z. Ikonić, V. Milanović, and D. Tjapkin, Appl. Phys. Lett. **54**, 247 (1989).